RSC Advances

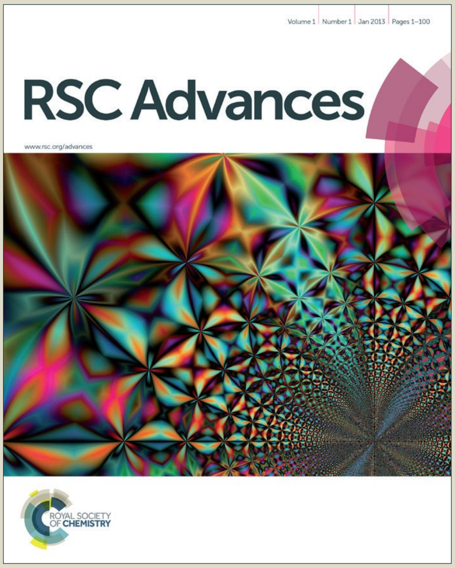

ROYAL SOCIETY OF CHEMISTRY

www.rsc.org/advances

Journal Name

ARTICLE

A convenient and efficient synthesis method to improve the emission intensity of rare earth ions doped phosphors: the synthesis and luminescent properties of novel SrO:Ce^{3+} phosphor

Received 00th January 20xx,
Accepted 00th January 20xx

DOI: 10.1039/x0xx00000x

www.rsc.org/

Jipeng Fu,[a,b] Su Zhang,[*,a] Tengfei Ma,[a,c] Yonglei Jia,[a,b] Ran Pang,[a] Lihong Jiang,[a] Da Li,[a] Haifeng Li,[a,b] Wenzhi Sun,[a,b] Chengyu Li[*,a]

Convenient and efficient synthesis methods to improve the emission intensity of rare earth ions doped phosphors are relatively less. In this work, a simple and modified solid-state reaction is proposed. The approach can strongly improve the reaction temperature and overcome the limitation of the harsh requirement. The advantages are generated from the substitute of solid-solid interface for solid-gas interface. Using the method, a novel Ce^{3+} doped SrO phosphor with an enhancive bright cyan emission is prepared. The photoluminescent properties of SrO:Ce^{3+} are first reported. This work will provide valuable clues for synthesizing many other ions doped functional materials besides rare earth ions doped luminescent materials.

Introduction

Doping is the most important and efficient method to endow hosts with various functions. For optical materials, the doped rare earth ions acting as the isolated active center can emit rich and colorful lights.[1-3] For many other functional materials, such as magnetic material, thermoelectric materials, superconductor, electrode material, etc., doped ions will also intensively improve or affect the performances and properties of them.[4,5] There are some techniques to introduce doping ions into a host. The familiar and common ones are ion implantation, thermal diffusion, chemical vapor deposition, ect.[6,7,8] Among them, high temperature solid state reaction, utilizing the diffusion of ion at high temperature, is the most simple and efficient ways to produce doped materials, though it has been used for many years. However, for the hosts which have relative lower physicochemical stability, the reaction at high temperature must be protected in an atmosphere of inactive gas, such as nitrogen, argon, to avoid the effects from oxygen, carbon dioxide, water vapour in air. And this will doubtless increase the cost and complexity of the production.

SrO is an important basic chemical raw materials. Recently, doped SrO itself demonstrates many charming properties in the fields of optical, display and magnetic materials. For example, doped SrO crystal shows the properties of new candidates for transparent and half-metallic ferromagnetic DMSs (diluted magnetic semiconductors).[9] Satoru et al investigate the sputtering yield of SrO barrier coatings under He^+, Ar^+, and Kr^+ ion beams in plasma display panel.[10] Moreover, the photoluminescence (PL) of Eu^{2+} and Eu^{3+} in SrO are reported. [11-13] Fu et al. shows the long-lasting phosphorescence in Eu^{3+} and B codoped SrO.[14,15]

Despite the widely potential application of doped SrO, the simple and convenient method to directly synthesize various ions doped SrO is still less, especially for rare earth ions doped SrO at high temperature. Though it is known that the melting and boiling point of SrO is about 2600 °C and 3200 °C, respectively,[16] if heating the SrO above 1400 °C in air, the SrO will practically 'volatilize'.(The photos are shown in Figure 1s) It is probably due to the reaction between SrO and air at high temperature, because the thermodynamic parameters mentioned above of SrO are measured in argon atmosphere.[17] So far, several papers investigate the rare earth ions doped SrO, but the reaction temperature is relatively low and the high temperature solid state reaction (SSR) is not reported. Mari[13] observed the photoluminescence of Eu^{3+} in SrO prepared by combustion synthesis method with further heating to 1000 °C. R. W. Reynolds and L. A. Boatner[18] obtained the single crystals of Ce^{3+} doped SrO by an arc-fusion process. Due to the representative characters of Ce in rare earth ions, we choose CeO_2 as the raw material. A simple and convenient synthesizing method of Ce^{3+} doped SrO is proposed. Its photoluminescent properties are studied.

Experimental

Sample Preparation. In this modified SSR, $SrCO_3$ (99.9%), SiO_2 (99.9%), (99.9%), CeO_2 (99.99%) were employed as raw

---

[a] State Key Laboratory of Rare Earth Resources Utilization, Changchun Institute of Applied Chemistry, Chinese Academy of Sciences, Changchun 130022, Peoples R China.Email: Zhangsu@ciac.ac.cn, cyli@ciac.ac.cn

[b] University of Chinese Academy of Sciences, Beijing 100049, Peoples R China.

[c] College of material science and engineering, jililn Jianzhu University, changchun 130118, Peoples R China.

materials. At first, $SrCO_3$ and CeO_2 were mixed well as stoichiometric ratio in an agate mortar for 30 min. Then, $SrCO_3$ and SiO_2 were also mixed homogeneously in an agate mortar at molar ratio of 3:1. The mixed powder of strontium carbonate and silica plays a key role in this method. Doped and undoped SrO phosphors were synthesized by putting starting materials in the middle of the mixed powder as sandwich structure and they were placed in a corundum crucible with a lid. After that, the crucible was placed in a box type electric-resistance furnace with silicon-molybdenum bar at a high temperature for a certain time. Therefore, it is vividly called interlayer solid-state reaction in this paper, ISSR for short. After sintered, the products were stripped out from the middle of the sandwich and grinded, waiting for a post-calcination in a selective condition. For $SrO:Ce^{3+}$ sample, it should be annealed at 550 °C for 1 h in CO atmosphere to reducing Ce^{4+}. The SrO powder crystal is chemical unstable to H_2O and CO_2, should be carefully handled.

For comparison, the Ce doped SrO phosphors were also prepared by a tradition solid-state reaction (SSR) without covering the mixed powder. In addition to this, the other treatment processes were the same.

Measurements and Characterization. The structure of the samples was identified by powder X-ray diffraction (XRD) analysis (Bruker AXS D8), with graphite-monochromatized Cu Kα radiation (λ = 0.15405 nm) operating at 40 kV and 40 mA. The absorption spectra were obtained by a UV-visible spectrophotometer (Hitachi U4100) using $BaSO_4$ as a reference. The measurements of photoluminescence (PL) and photoluminescence excitation (PLE) spectra were performed using a Hitachi F7000 spectrometer equipped with a 150 W xenon lamp under a working voltage of 700 V. The excitation and emission slits were set respectively at 1.0 nm and 2.5 nm. The luminescence decay curve was obtained from a Lecroy Wave Runner 6100 digital oscilloscope (1 GHz) using a tunable laser (pulse width = 4 ns; gate = 50 ns) as the excitation source (Continuum Sunlite OPO). The quantum efficiency yields were analyzed with a PL quantum-efficiency measurement system (C9920-02, Hamamatsu Photonics, Shizuoka, Japan) by a 150 W xenon lamp. All of the measurements were performed at room temperature.

Results and discussion

Synthesis mechanism. SrO has a typical crystal structure, because all the normal alkaline-earth oxides with MO formula have the NaCl crystal structure except for BeO. Although, SrO has a very high melting point, the traditional SSR is hard to be employed to synthesize rare earth ions doped SrO, because the high reaction temperature and long processing time in air result in the 'volatilization' of SrO. The single quotation marks mean that it's not a simple physical process. A number of complicate chemical reactions may cause the melting and disappearing of SrO when above 1400 ^{o}C as shown in Scheme 1 left. It should be mentioned that Ce^{3+} doped SrO can also be synthesized by traditional SSR, but by the traditional SSR the PL emission intensity of $SrO:Ce^{3+}$ is quite weak (shown in Figure 6). This phenomenon may be due to the inferior doping process of Ce ion at lower temperature.

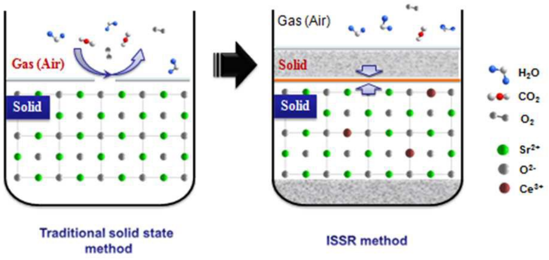

Scheme 1. The sketch map of the traditional solid state reaction (left) and ISSR method (right).

In the ISSR method, the starting materials are first heated at 1200 ^{o}C for 2 hours. At this temperature the $SrCO_3$ can be decomposed into SrO and CO_2. And then the furnace is further heated up to 1530 ^{o}C and kept for 4 hours. With increasing the temperature the reaction and diffusion rate between CeO_2 and SrO will both enhanced. This is the main cause of the higher PL emission of Ce^{3+} doped SrO samples synthesized by ISSR method. Therefore, there are three key effects of the covering layer made from $SrCO_3$ and SiO_2 mixture in ISSR method (Scheme 1 right). First, the coating makes the solid-solid interface instead of the solid-gas interface. The coating can efficiently exclude the active molecules in air to prevent the SrO from volatilizing. Second, the coating can protect the starting materials from shock of thermal convection in furnace. Third, $SrCO_3$ and SiO_2 mixture will form a stable silicate compound at a high temperature. The target product SrO is difficult to react with this silicate compound. Thus, due to the well doping process of Ce ions at a relatively higher temperature, a better Ce ions emission in SrO can be obtained.

Additionally, it is common that reducing the particle size of the raw materials will be of great benefit to the diffusion of the ions, such as the sol-gel method,[19] combustion synthesis,[20] and co-precipitation method,[21] nevertheless a post-calcination process is still needed for various synthesis methods, because in the process of doping ions, the main factors, chemical reaction, diffusion, crystal growth and defect adjustment are

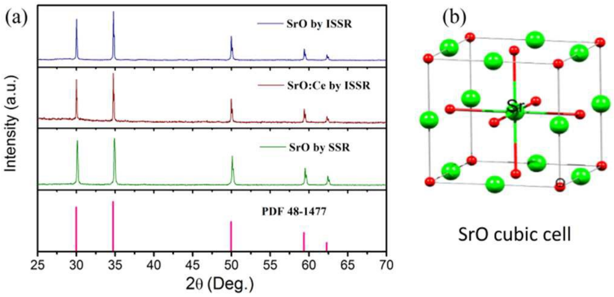

Figure 1. (a) XRD patterns of as-synthesized SrO: $0.01Ce^{3+}$, SrO and the standard pattern of SrO (PDF#48-1477). (b) A schematic representation of the geometric structure of the SrO cubic cell.

all intensively affected by temperature. Hence, the ISSR method may still have the strong attraction of convenient operation and low cost in synthesizing ions doped materials.

Crystal Structure and emission color of Ce^{3+} doped SrO. The typical XRD patterns of undoped and Ce^{3+} doped SrO phosphors synthesized by ISSR and traditional SSR, as well as the standard pattern of SrO, are shown in Figure 1. All XRD patterns are found to agree well with the cubic SrO (space group: Fm-3m). The XRD patterns indicate that at a high temperature the raw material $SrCO_3$ will easily be decomposed into SrO, and most importantly, it is shown that the special high temperature of ISSR did not generate any impurity or induce significant changes in the host structure, as well as the doped Ce^{3+} ions. Hence, it is possible that the better PL emission properties of Ce^{3+} may originate from the well diffusion of Ce^{3+} ions in SrO and the better crystal growth and better crystal defect adjustment process of SrO at a relatively high temperature. Figure 2 shows the photograph of Ce^{3+} doped and undoped SrO synthesized by ISSR under a 254 nm UV light. A bright cyan can be seen.

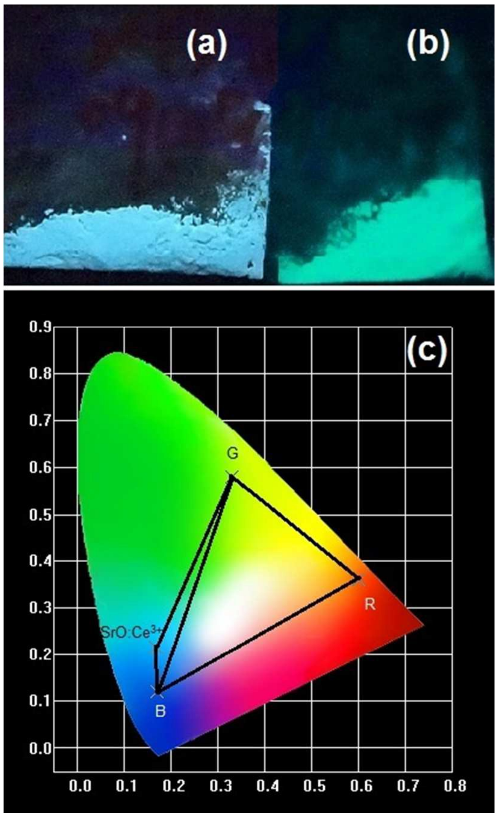

Figure 2. The photograph of SrO: Ce^{3+} (a) and SrO (b) synthesized by ISSR under 254 nm UV light. (c) CIE coordinates of SrO:Ce^{3+} and SrO phosphor in a CIE 1931 chromaticity diagram, together with commercial RGB phosphors: Y_2O_3:Eu^{3+} (R),Y_2SiO_5:Tb^{3+} (G) and Y_2SiO_5:Ce^{3+} (B).

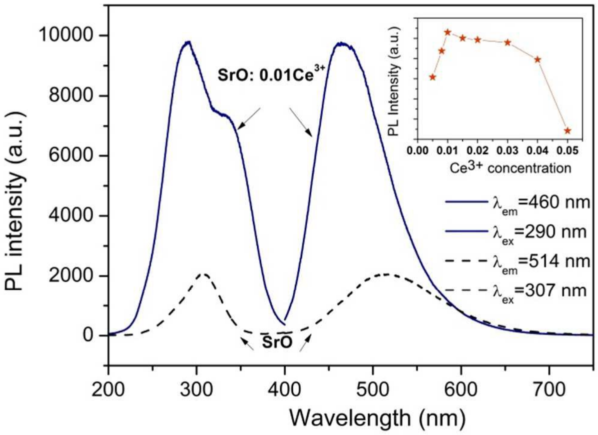

Figure 3. PL (solid curve) and PLE (dash curve) spectra of SrO and SrO: $0.01Ce^{3+}$. The inset shows PL integrate intensity of SrO: xCe^{3+} (x=0.005-0.05).

The PL properties of Ce^{3+} doped and undoped SrO synthesized by ISSR. The PL spectra of SrO and SrO:Ce^{3+} synthesized by ISSR are presented in Figure 3. The emission spectrum of SrO:Ce^{3+} shows a broad peak located around 460 nm under the excitation of 290 nm. The emission is attributed to the $^5d_1 \rightarrow {}^4f_1$transition of the Ce^{3+} ions. Although the $^5d_1$ state of Ce^{3+} will split into at most 5 levels, in the room temperature PL excitation spectrum only two peaks can be recognized, which are located at about 288 and 338 nm.

From the emission spectrum of SrO:Ce^{3+}, the color coordinates are calculated to be (0.168, 0.216). Generally, RGB (red, green and blue) tricolor phosphors are used in 3D display devices, such as field emission displays (FEDs) and plasma display panels (PDPs). However, the introduction of a cyan-emitting phosphor should enlarge the display gamut, and make the images of the devices more colorful and natural (Figure 2c).[22,23] Importantly, the bright cyan emission implies that the ISSR can dower host with exceptional characters.

It is also interesting that the undoped SrO can also give an emission of green. Under 307 nm excitation, the PL spectrum of SrO shows abroad band peaked at 514 nm. The color coordinates are (0.28, 0.44) (the photograph is shown in Figure 2). The green emission of SrO is attributed to lattice defects and deformed crystals of pure SrO not to impurities.[12,24-27] Similar host emissions are also reported in CaO, MgO and BaO.[26] And the quantum efficiency of Ce doped and undoped SrO are about 20% and 10%, respectively.

The insert of Figure 3 shows the emission intensity as a function of the doping content. For those samples with higher Ce^{3+} dopant content, concentration quenching was observed. The optimal Ce^{3+} dopant content was found to be 1 mol%, from which it is possible to calculate the critical distance (R_c) for concentration quenching using the following equation:[28]

$$R_c \approx 2\left(\frac{3V}{4\pi x_c N}\right)^{1/3} \quad (1)$$

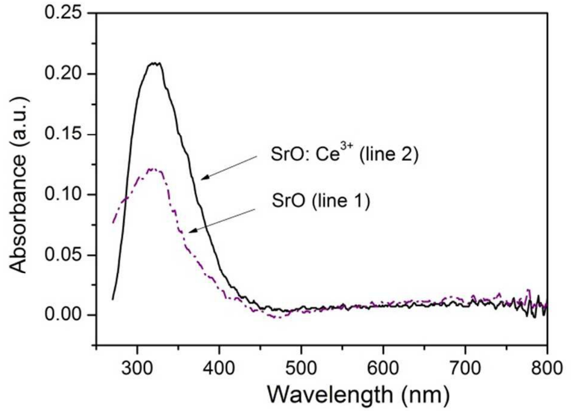

Figure 4. UV-visible absorption spectra of un-doped SrO (line 1) and Ce^{3+} doped SrO (line 2) measured at room temperature.

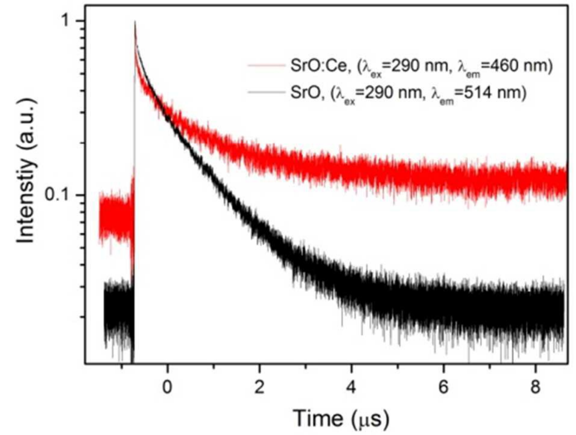

Figure 5. The luminescence decay curves of SrO: $0.01Ce^{3+}$ excited at 290 nm and monitored at 460 nm, SrO excited at 290 nm and monitored at 514 nm.

Where V is the volume of the unit cell, x_c is the critical concentration of the activator ion, and N is the number of total Ce^{3+} sites per unit cell. In SrO, N=4, V=136.9 Å^3, and the critical concentration x_c is about 0.01 in our system. Based on equation (1), the critical distance R_c is calculated to be 18.7 Å. The large R_c means the large critical concentration of dopant.

The UV-visible absorption spectra are employed to investigate their absorption of light. The absorption spectra of the undoped and Ce^{3+} doped SrO shows that both the samples have no absorption above 450 nm (Figure 4). It is demonstrated that the absorption of Ce^{3+} ions is overlapped with the host absorption at 320 nm.

Figure 5 shows the luminescence decay curves of the SrO:Ce^{3+} and SrO phosphors excited at 290 nm, which provide further insight into the luminescent centers of SrO and SrO: Ce^{3+}. Luminescent lifetime of SrO is calculated on the assumption that the observed decay curves are the sum of several first order decay curves.[26] The decay curves of undoped SrO can be well fitted with a second-order exponential equation,[29]

$$I=A_1\exp(-t/\tau_1) + A_2\exp(-t/\tau_2) \qquad (2)$$

Where I is the luminescence intensity at time t; A_1 and A_2 are constants, and τ_1 and τ_2 is defined as the rapid and slow luminescent lifetime. The lifetime values are determined to be 1.03 μs and 0.105 μs for SrO. These values are smaller than that of SrO in Coluccia's results,[26] which may be due to the quenching of PL from surface absorption, because the host emission is attributed to the presence of local surface states. Considering the overlap of the host and the Ce^{3+}emission, we try to fit the decay curve of SrO:Ce^{3+} with a third-order exponential equation. The lifetime values are calculated to be 1.75 μs, 0.407 μs and 0.022 μs. We do not presume too much on the reliability of these values. However, it is really possible that the orders of magnitude of the values are reliable. Figure 5 shows intuitively that in the initial period of the curve of SrO:Ce, the decay is faster than that of SrO. Because the lifetime of d-f transition of Ce^{3+} is nanosecond, the calculated lifetime value 0.022 μs (22 ns) of SrO: Ce may be attributed to the d-f transition of Ce^{3+}. The short decay time of the order of μs can avoid cross-talk for displays (within about 2 ms). Hence, taking into account the suitable emission color and the extremely short life time, the potential application of SrO:Ce^{3+} in 3D display devices is anticipated.

The emission intensity of SrO:Ce synthesized by ISSR and traditional SSR. In order to compare the emission intensity of SrO:Ce synthesized by different methods, the PL emission spectrum is measured (The SEM photographs of the samples are shown in supporting information, Figure 2s). Figure 6 shows that the spectra of the samples share a similar peak type, which is due to the transitions from d level to $^2F_{7/2}$ and $^2F_{5/2}$ of Ce^{3+}. However, the intensity of the emission varies considerably. The emission intensity of SrO:Ce synthesized by ISSR is obviously stronger than the sample synthesized by traditional SSR, even if at a relatively lower synthesis temperature.

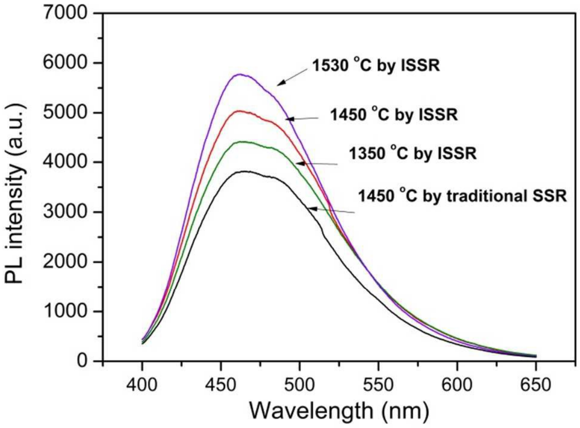

Figure 6. PL emission spectra of SrO:$0.01Ce^{3+}$ synthesized at different temperature (1530 °C, 1450 °C, 1350 °C) by ISSR approach and the spectrum of the sample obtained at 1450 °C prepared by tradition solid-state reaction.

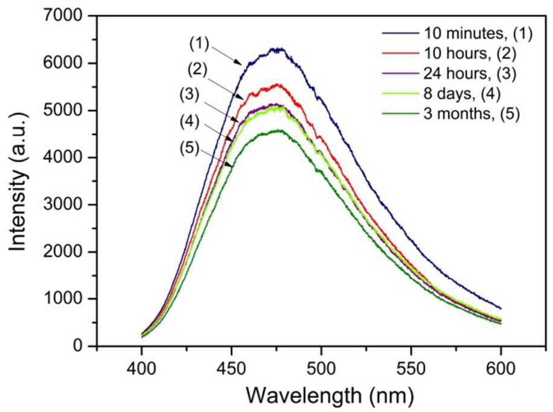

Figure 7. PL spectra of SrO: 0.01Ce^{3+} exposed in air from 10 minutes to 3 months.

The emission intensity of the products was strongly affected by the reaction temperatures, because temperature will affect the depth and impurity concentration of doping. For the samples synthesized by traditional SSR, 1450 °C is the highest temperature it can reach. The emission of this sample is quite low when compared with the sample synthesized by ISSR at 1350 °C. When the reaction is carried out at a higher temperature (e.g., 1450 °C, 1530 °C), the emission intensity is increased simultaneously. When the synthesis temperature reaches 1530 °C, the emission intensity of the sample from ISSR method is 50 percent higher than the sample from traditional SSR. The intensive luminescence of Ce^{3+} ions in SrO synthesized by ISSR can be attributed to the well diffusion and better interaction between host and doping ions.[24,25] The reducing of crystal defects due to the higher reaction temperature may be another cause. Due to the complexity of solid state reaction, the possibilities need more experimental confirmations.

The stability of Ce^{3+} doped SrO synthesized by ISSR. One intuitively knows that SrO is chemically unstable in air. Here, the stability of Ce^{3+} doped SrO synthesized by ISSR is investigated. The time ageing spectrum of sample is introduced (Figure 7). Figure 7 shows that at the initial 24 hours, the emission intensity of SrO: Ce^{3+} decreased intensively. However, when the sample is exposed more than 24 hours, the change of the emission intensity is not marked. SrO is truly unstable in air. When the sample was putted in air for 24 hours, the sample generally expanded. And the XRD measured after it was exposed in air for 24 hours (Figure 3s) shows that there are some peaks which belong to $Sr(OH)_2$ and $SrCO_3$. However in this case, the shapes of the PL luminescent spectra are not changed, which indicate that the crystal structure of the luminescent part of the sample is not changed, because a slight change of the coordination environment well cause the remarkable variety of the emission spectrum of the Ce^{3+}.[30] Therefore, we deduce that the decomposer may provide a shielding environment, which prevents the core structure of the phosphor from future carbonation and hydrolysis. Hence, deliberate attempts to modify the surface may engender a good phosphor.

Conclusions

A convenient modified solid state reaction method, ISSR method, to obtained Ce^{3+} doped SrO were reported. Using the ISSR method, the reaction temperature of doping Ce^{3+} into SrO can be increased as much as 1530 °C in air. An enhanced cyan Ce^{3+} emission is observed, which is due to the better diffusion of Ce ion at a high temperature. Most importantly, the results of the investigations indicate that ISSR may provide a new concept and strategy for conveniently synthesizing other ions doped functional materials.

Acknowledgements

The authors are grateful to the financial aid from the Hong Kong, Macao and Taiwan Science and Technology Cooperation Special Project of China MOST (Grant No. 2014DFT10310), Program of Science and Technology Development Plan of Jilin Province of China (Grant No. 20140201007GX), the National Basic Research Program of China (973 Program, Grant No.2014CB643801), National Natural Science Foundation of China (Grant Nos. 51102229, 51402288, 21401184).

Notes and references

1 Y. R. Sun, N. C. Giebink, H. Kanno, B. W. Ma, M. E. Thompson, S. R. Forrest, *Nature*, 2006, **440**, 908-912.
2 R. T. Wegh, H. Donker, K. D. Oskam, A. Meijerink, *Science*, 1999, **283**, 663-666.
3 M. Yu, J. Lin, Z. Wang, J. Fu, S. Wang, H. J. Zhang, Y. C. Han, *Chem. Mater.*, 2002, **14**, 2224-2231.
4 J.M.D. Coey, M. Venkatesan, C.B. Fitzgerald, Nat Mater, 2005, **4**, 173-179.
5 A.S. Sefat, *Phys. Rev. Lett.*, 2008, **101**, 117004.
6 R. J. Hong, J. B. Huang, H. B. He, Z. X. Fan, J. D. Shao, *App. Surface Sci.*, 2005, **242**, 346-352.
7 L. E. Shea, J. Mckittrick, O. A. Lopez, E. Sluzky, *J. Am. Chem. Soc.*, 1996, **79**, 3257-3265.
8 H. C. Lu, G. S. Yi, S. Y. Zhao, D. P. Chen, L. H. Guo, J. Cheng, *J. Mater. Chem.*, 2004, **14**, 1336-1341.
9 K. Kenmochi, *J. Phys. Soc. Japan*, 2004, **73**, 2952-2954.
10 S. Yoshimura, *Japanese J. Appl. Phys.*, 2012, **51**, 08HB02.
11 N. Yamashita, *J. Electrochem. Soc.,* 1993, **140**, 840-843.
12 N. Yamashita, *J. Lumin.*, 1994, **59**, 195-199.
13 B. Mari, K.C. Singh, M. Moya, I. Singh, H. Om, S. Chand, *Opt. Mater.,* 2012, **34**, 1267-1271.
14 J. Fu, *Electrochem. Solid St. Lett.,* 2000, **3**, 350-351.
15 P. A. M. Berdowski, M. J. J. Lammers, G. Blasse, *J. Chem. Phys.,* 1985, **83**, 476-479.
16 D. Risold, B. Hallstedt, L. J. Gauckler, *Calphad*, 1996, **20**, 353-361.
17 K. Irgashev, V.D. Tarasov, V. Y. Chekhovskoi, *High Temp.*, 1985, **23**, 86-91.
18 R. W. Reynolds, Y. Chen, L. A. Boatner, M. M. Abraham, *Phys. Rev. Lett.,* 1972, **29**, 18-21.
19 B. Yan, H. J. Zhang, S. B. Wang, J. Z. Ni, *Mater. Chem. Phys.*, 1997, **51**, 92-96.

20 J. Mckittrick, L. E. Shea, C. F. Bacalski, E. J. Bosze, *Dispalys*, 1999, **19**, 169-172.
21 W. Pan, G. L. Ning, X. Zhang, J. Wang, Y. Lin, J. W. Ye, *J. Lumin*, 2008, **128**, 1975-1979.
22 C. Liu, S. Zhang, Z. Liu, H. Liang, S. Sun, Y. Tao, J. Mater. Chem. C, 2013, **1**, 1305-1308.
23 M. Xie, H. Liang, Q. Su, Y. Huang, Z Gao, Y. Tao, Electrochem. Solid-State Lett., 2011, 14, J69-J72.
24 X. G. Peng, M. C. Schlamp, A. V. Kadavanich, A. P. Alivisatos, *J. Am. Chem. Soc.,* 1997, **119**, 7019-7029.
25 T. R. Wang, P. Li, H. R. Li, *ACS Appl. Mater. Interfaces*., 2014, **6**, 12915-12921.
26 S. Coluccia, A.M. Deane, A.J. Tench, J. Chem. Soc., Faraday Transactions 1: Physical Chemistry in Condensed Phases, 1978, **74**, 2913-2922.
27 Y. Chen, *Philosophical Magazine*, 1975, **32**, 99-112.
28 W.B. Im, *Chem. Mater.*, 2010, **22**, 2842-2849.
29 R. Pang, C. Y. Li, S. Zhang, Q. Su, *Mater. Chem. Phys*., 2009, **113**, 215-218.
30 X. Ding, H. Liang, D. Hou, S. Jia, Q. Su, S. Sun and Y. Tao, *J. Phys. D: Appl. Phys.*, 2012, **45**, 365301.